Available online at www.sciencedirect.com
ScienceDirect
Applied Catalysis A: General 321 (2007) 58–70
APPLIED CATALYSIS A: GENERAL
www.elsevier.com/locate/apcata

Influence of the preparation method on the activity of phosphate-containing CoMo/HMS catalysts in deep hydrodesulphurization

R. Nava [a,*], J. Morales [a,b], G. Alonso [c], C. Ornelas [c], B. Pawelec [d], J.L.G. Fierro [d]

[a] *CFATA, UNAM, Campus UNAM Juriquilla, Querétaro 76000, Mexico*
[b] *PCEIM, Instituto de Investigaciones en Materiales, UNAM, D.F., Mexico*
[c] *CIMAV, S.C., Chihuahua, Mexico*
[d] *Instituto de Catálisis y Petroleoquímica, CSIC, Cantoblanco, Madrid, Spain*

Received 27 September 2006; received in revised form 12 January 2007; accepted 15 January 2007
Available online 25 January 2007

Abstract

Phosphate-containing hexagonal mesoporous silica (P/HMS) materials were used as supports of hydrotreating CoMo catalysts. Two series of catalysts were prepared by sequential and simultaneous impregnation of P/HMS substrates with cobalt and molybdenum salts solutions. Both bulk and surface structures of calcined and sulphided samples were determined by several techniques (S_{BET}, XRD, UV–vis, TPD-NH_3, TPR, FTIR of adsorbed NO and pyridine, HRTEM and XPS). The activity of P-containing CoMo catalysts was examined in hydrodesulphurization (HDS) of dibenzothiophene (DBT) and compared to that of a conventional commercial CoMo/Al_2O_3 catalyst. It was found that the dispersion of oxide and sulphide Co and Mo species depends on the presence of phosphate and also on the sequence of Co and Mo incorporation being co-impregnation more favourable than sequential impregnation. HRTEM analysis of sulphided samples (673 K) showed that larger stacking degree of MoS_2 phase and better dispersion of Co and Mo species are achieved by co-impregnation. Activity tests revealed that sequential incorporation of Mo and Co is less effective for S-removal from DBT than co-impregnation. Contrary to sequential impregnation, the presence of P_2O_5 (up to 1.5 wt.%) on support surface enhanced S removal from DBT on the catalysts prepared by co-impregnation but the selectivity in this reaction was not influenced by phosphate and catalyst's preparation method. A close parallelism between active phase surface exposure and catalytic response was found.

Keywords: CoMo catalysts; Phosphorous; HMS support; HDS; DBT

1. Introduction

Government regulations call for the production and use of more environmental friendly fuels with lower contents of sulphur and aromatics. The European Union intends to reduce sulphur content to 10 ppm by 2009 for diesel and gasoline [1]. Since several decades ago the mixed transition metal sulphides (TMS) such as Ni(Co)-Mo supported on high surface area γ-Al_2O_3 material are commercially applied catalysts for the sulphur removal from heterocyclic compounds present in heavy oil fractions. However, the demand for lower sulphur content in fuels requires utilization of new materials as catalyst supports.

In order to improve the catalyst properties, the phosphorous addition to commercial Co(Ni)Mo catalysts is a common practice. The beneficial effect of phosphate on the hydrodesulphurization (HDS) activity of sulphided Co(Ni)Mo/Al_2O_3 catalysts was claimed in few patents [2–4]. The effect of the phosphate incorporation on the activity of Al_2O_3-supported Mo and NiMo catalysts was studied for HDS of model compounds such as thiophene [5–14], dibenzothiophene [15], methyl-substituted DBT [16,17] as well as with real feeds such as gas oil [15]. However, employing model compounds such as thiophene and dibenzothiophene (DBT), the results were contradictory [5–14]. Thus, no detectable promotion effect of phosphorus in the HDS of thiophene was reported for MoP/Al_2O_3 catalysts [11–14]. Similarly, phosphate-modified catalysts showed a lower activity than the P-free ones in HDS of DBT and real feeds [15,16]. Several proposals have been

* Corresponding author. Tel.: +52 555 623 4143; fax: +52 555 623 4165.
E-mail address: rufino@fata.unam.mx (R. Nava).

0926-860X/$ – see front matter
doi:10.1016/j.apcata.2007.01.038

advanced in literature in order to explain the HDS activity improvement over alumina-supported catalysts containing phosphate. The most frequently proposed explanations are: (i) phosphate acts as a second promoter [18]; (ii) enhancement of solubility of molybdate by formation of phosphomolybdate complexes which led to easier catalyst preparation [8,19]; (iii) formation of lower amount of inactive Co/Ni species [8,20]; (iv) improved dispersion of the active phase [7,8,21,22]; (v) formation of stacked layers easier to sulphide [9,23]; (vi) lower catalyst deactivation during on-stream operation [24].

The influence of the catalyst preparation method on the structure of phosphorus containing CoO-MoO_3/Al_2O_3 catalysts was studied by Moulijn and co-workers [25,26]. The authors found that the influence of P on the distribution of the Mo species depends on the P content and the sequence of impregnation (co-impregnation of Co, Mo and P or sequential impregnation being P incorporated first). The authors observed that, irrespectively of the order of P incorporation, the Co interaction with MoO_3 and $AlPO_4$ species forming Co-Mo-O-P phase occurs. The reducibility of the Co^{2+}-ions in this phase was decreased compared to the reducibility of these ions in the Co-Mo-O phase because the stronger polarization of the Co–O bond by P^{5+} [25]. Moreover, the sulphidation of Co/Ni was found to be more difficult due to an interaction between the metal atoms and aluminium phosphate phase formed on the alumina support surface [26]. Interestingly, the ^{95}Mo NMR study of CoMo/γ-Al_2O_3 catalysts performed by Edwards and Ellis indicated the catalysts prepared by sequential impregnation showed larger lines broadening than those prepared by co-impregnation [27]. This indicate that cobalt in the former systems might form isolated clusters whereas the formation of mixed Co-Mo phases during co-impregnation occurs. Employing the quantitative ^{31}P and ^{27}Al solid state NMR, Kraus and Prins [28] studied the effect of impregnation procedures on the structures of oxidic phosphorus-containing NiMo/Al_2O_3 and CoMo/Al_2O_3 catalysts. In case when the Co/Ni and phosphorus were separately deposited on the catalyst surface, the aluminium phosphate ($AlPO_4$) was detected. The formation of this phase was found to be favoured in nickel-containing samples whereas the creation of Co–Mo–P compounds was favoured in samples containing cobalt [28].

Recently, for hydrotreating catalysts a large variety of new mesoporous silica-based carriers, such as MCM-41 and HMS, etc., have been intensively studied [29–34]. In comparison to MCM-41, the textural characteristics of hexagonal mesoporous materials (HMS) have certain advantage due, in part, to its larger textural mesoporosity and wormhole mesostructure which offers better transport for reactants and products. Contrary to alumina, the formation of silica phosphates on this siliceous material seems unlikely because silica surface contains OH groups which are less reactive than those on Al_2O_3 [35]. Indeed, the high temperature needed (above 873 K) in silica may cause shrinkage by forming phosphosilicate [36]. Thus, one might expect rather that the PO_4^{2-} anions on surface of silica might react with Co and/or Mo forming respective phosphates.

Within the above framework, this work was undertaken with the aim to examine the influence of both: the catalyst preparation method (sequential impregnation versus co-impregnation) and the presence of phosphate species on the structures of calcined and sulphided CoMo catalysts supported on hexagonal mesoporous silica (HMS) and how these structures determine the performance for the HDS reaction of DBT. The physicochemical properties of pure supports and CoMo catalysts has been evaluated by various techniques (N_2 adsorption–desorption at 77 K, XRD, UV–vis DRS, TPD-NH_3, TPR, FTIR of NO, XPS, HRTEM) and their activity compared with those of a conventional commercial CoMo/Al_2O_3 catalyst.

2. Experimental

2.1. Preparation of supports and catalysts

The HMS molecular sieve was prepared at room temperature following a procedure similar to that reported by Zhang et al. [37]. Tetraethylorthosilicate (TEOS, 98%, Aldrich) was used as the neutral silica precursor, dodecylamine (DDA, 98%, Aldrich) and mesitylene (MES, 97%, Aldrich) were used as a neutral structure director and swelling agent, respectively. In a typical synthesis the surfactant (DDA) and the corresponding amount of water were mixed at vigorous stirring to obtain a homogeneous solution. MES was added to the surfactant solution and stirred for 15 min. Then, TEOS was added to the surfactant-auxiliary solution and the mixture was allowed to react under stirring at room temperature for about 20 h. The solid residue was filtered, exhaustively washed with distilled water and dried first in air at room temperature and then at 373 K for 24 h. Finally, the sample was calcined at 813 K in air for 6 h. The absence of remaining surfactant in the synthetized support was confirmed by XPS technique. The phosphate-modified HMS was achieved via incipient wetness impregnation of parent HMS material with aqueous solutions of H_3PO_4 of appropriate concentrations to obtain P/HMS substrates with P_2O_5 loadings of 0.5, 1.0, 1.5, 2.0 wt.%. After water evaporation at room temperature, the solid was dried at 383 K overnight and then calcined at 773 K for 3 h.

Two series of CoMo catalysts were prepared by sequential and co-impregnation via incipient wetness method. Employing sequential impregnation, the molybdenum salt (ammonium heptamolybdate tetrahydrate, Aldrich) was introduced first. Then the Mo/P/HMS (and Mo/HMS reference) impregnates were dried overnight at 383 K in air and then calcined for at 773 K in air for 3 h. Finally, the Mo-loaded samples were then impregnated with a cobalt salt (cobalt (II) nitrate hexahydrate, Aldrich, 98%). The concentrations were calculated to achieve Mo and Co loadings of 10.0 and 3.0 wt.%, respectively, which correspond to a Co:Mo molar ratio of 1:3. Drying and calcination were the same than above. Co-impregnated catalysts were prepared in a similar manner but adding simultaneously both molybdate and cobalt salts to impregnant solution. The catalysts will be referred to hereafter as Co/Mo/P(x)/HMS and CoMo/P(x)/HMS for sequentially impregnated and co-impregnated samples, respectively (x refers to P_2O_5 loadings of 0.5, 1.0, 1.5 or 2.0 wt.%.

2.2. Catalysts characterization

The BET specific surface areas were determined from nitrogen adsorption/desorption isotherms at 77 K using an Autosorb 1 (Quantachrome) equipment. Before adsorption, the samples were degassed under argon flow at 473 K for 2 h. The error bar in BET measurements was ±3%.

Powder X-ray diffraction patterns of the supports and catalysts were recorded on a DMAX 2100 Rigaku diffractometer using Cu Kα radiation in the 2θ range of 0.5–80°.

The UV–vis diffuse reflectance spectra of the oxide samples were recorded in the range of 200–700 nm at room temperature using a Varian Cary 3 UV–vis spectrometer equipped with an integration sphere. The respective support in each catalyst was used as a reference.

For high magnification TEM study, the sulphide (673 K) catalysts were crushed and ultrasonically dispersed in acetone at room temperature and then spread on a holey carbon-copper microgrid. TEM images were collected on a Joel TEM-3000F microscope operating at 300 kV.

The acidity of the supports was determined by temperature-programmed desorption (TPD) of ammonia using a Micromeritics 2900 equipment provided with a TCD and interfaced to a data station. The samples of 50 mg were degassed in a He flow (Air Liquide, 99.996%) at 383 K for 1 h. Then, the ammonia-saturation was performed with flowing 5% NH_3/He mixture at 400 K for 0.5 h. After equilibration in argon flow for 1 h at 353 K, the samples were heated at 10 K/min up to 1200 K, and the TCD signal of ammonia desorption was recorded.

The acidity of sulphided catalysts was followed by FTIR of adsorbed pyridine carried out on Nicolet 510 FTIR spectrophotometer. After sulphidation at 673 K, the samples were degassed at 723 K for 0.5 h and cooled to ambient temperature prior to contact with ca. 2 Torr of pyridine. Physically adsorbed pyridine was removed by degassing at 393 K for 1 h. More details are elsewhere reported [34].

TPR experiments were conducted on the Micromeritics 2900 equipment. Prior to reduction, the oxide catalysts (ca. 50 mg) were heated at a rate of 20 K/min up to a final temperature of 673 K, and kept for 2 h at that temperature under a flow of He to remove water and other contaminants. The catalysts were cooled to ambient temperature in the same flow of He; then reduced in flowing gas containing 10 vol.% H_2 in Ar at a total flow rate of 50 ml/min, and finally heated at a rate of 15 K/min up to a final temperature of 1300 K.

The FTIR spectroscopy of adsorbed NO was used to determine the relative dispersion and sulphidation degree of Co (and Mo) phases after in situ sulphidation at 673 K. Self-supporting wafers of the catalysts with thickness of 12 mg/cm^2 were prepared by pressing the powdered samples at a pressure of 7×10^3 kg/cm^2 for 10 min. The samples were degassed at 673 K for 2 h in an IR cell having greaseless stopcocks and KBr windows. Once the samples were cooled down to ambient temperature, they were exposed to 20 mbar of NO for 5 min and subsequently the spectrum was recorded on a Nicolet 510 FTIR spectrophotometer at a resolution of 4 cm^{-1}. Then the samples were degassed at 673 K for 2 h to remove adsorbed NO molecules and the spectrum of the catalyst was recorded. The net IR spectrum of the adsorbed NO was obtained by subtracting the spectrum of the sample degassed at 673 K from the one recorded upon adsorption of NO.

The X-ray photoelectron spectra of the ex situ sulphided (673 K for 4 h) catalysts were recorded on a VG Escalab 200R spectrometer equipped with a hemispherical electron analyzer and an Mg Kα ($h\nu$ = 1253.6 eV) X-ray source was used. The freshly sulphided CoMo catalysts were kept under *i*-octane in order to avoid exposure to air and then placed in a copper holder mounted on a sample-rod in the pre-treatment chamber of the spectrometer. The samples were degassed at 10^{-5} mbar and then transferred to the ion-pumped analysis chamber, where residual pressure was kept below 7×10^{-9} mbar during data acquisition. The binding energies (BE) were referenced to the C 1s peak (284.9 eV) to account for charging effects. The areas of the peaks were computed after fitting of the experimental spectra to Gaussian/Lorentzian curves and removal of the background (Shirley function). Surface atomic ratios were calculated from the peak area ratios normalized by the corresponding atomic sensitivity factors [38].

2.3. Catalytic activity

Prior to the catalytic test, the catalysts were sulphided at 673 K for 4 h under a H_2/H_2S gas flow (15%H_2S, v/v) at atmospheric pressure. HDS of DBT was carried out in a Parr model 4522 high-pressure batch reactor. One gram of the catalyst with particle size 0.25–0.3 mm was introduced in the reactor together with the reactant mixture (6.6 g of DBT in 150 ml of decaline; $[DBT]_o$ = 0.239 mol/L). The reactor was pressurized to 3.1 MPa with hydrogen and then heated to 623 K at a rate of 10 K/min. The stirring of the reaction mixture was sufficiently intensive to exclude external diffusion limitations (checked by varying amount of catalyst and the power of stirring (1000, 800 and 700 rpm). Samples for chromatographic analysis were taken during the course of each run to determine conversion-time dependence. Reaction run time was extended to 5 h. After reaction, the used catalyst was separated from the products by decantation. The reaction products were analyzed using a Perkin-Elmer Auto-system chromatograph with a 2.5 m long × 1/8 in. diameter packed column containing chromosorb W-AW 80/100 mesh 3% OV-17 (phenyl methyl silicone 50% phenyl) as a separating phase. Estimated error in activity measurements was ±2%.

3. Results

3.1. Textural properties of supports and catalysts

The specific surface areas of the bare supports and CoMo-loaded catalysts were calculated from the N_2 adsorption-desorption isotherms at 77 K (not shown here) by applying the BET equation [39]. The variation of BET specific area with the P_2O_5 content is shown in Fig. 1. BET areas of pure supports are rather high, somewhat around 900 m^2/g, and quite similar

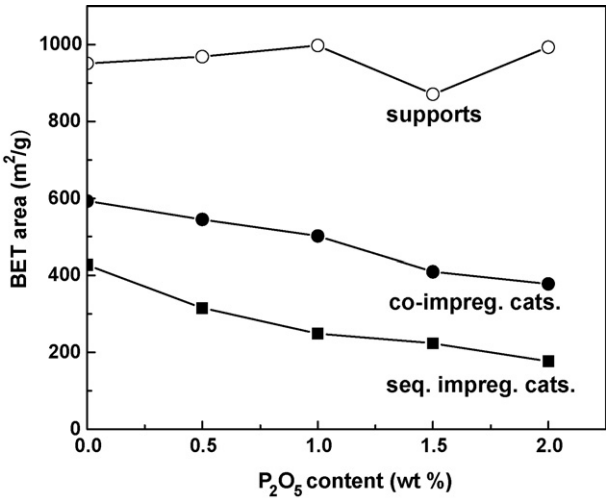

Fig. 1. BET area for bare supports and calcined CoMo catalysts vs. P_2O_5 content.

irrespective the P_2O_5 loading. The BET area drops strongly upon incorporation of CoMo phases. This drop depends on both preparation method and P_2O_5 loading and is much larger for the catalysts prepared by sequential than by co-impregnation.

Fig. 2 shows the pore size distributions, calculated by the BJH method to the desorption branch of the nitrogen isotherms, of the plain supports and all the calcined catalysts. Considering the relatively large average pore size of the supports (see Fig. 2), one may expect that aqueous solutions of ammonium heptamolydate (AHM) may penetrate the inner structure of mesoporous HMS material. Thus, the significant drop in the BET area observed for the catalysts prepared by sequential impregnation is probably due to the pore occlusion by the formerly deposited molybdenum oxide species and/or the occupation of the pore walls by MoO_3. Similarly, irrespectively of the catalyst preparation method, the pore entrance blocking by P_2O_5 phases located on the support surface may explain the additional decrease in BET surface area raising P_2O_5 content. This conclusion is corroborated by a larger average pore size of the catalysts prepared by sequential impregnation with respect to those prepared by co-impregnation (see Fig. 2(b and c)). The narrower and more uniform pore size distribution of the catalysts prepared by co-impregnation with respect to those prepared by successive impregnation suggest that the supported species are more uniformly distributed on the former than on the latter. The bulk Mo/Si and Co/Si atomic ratios calculated from the nominal metal oxides content are compiled in Table 2. For all catalysts, these values are much larger than those obtained from XPS measurements indicating that precursors of the active phases are mainly located within the inner catalyst structure.

3.2. Acid properties of the pure supports and sulphided catalysts

Temperature-programmed desorption of ammonia was carried out in order to compare the acidity of plain HMS material before and after modification by phosphate. The TPD-

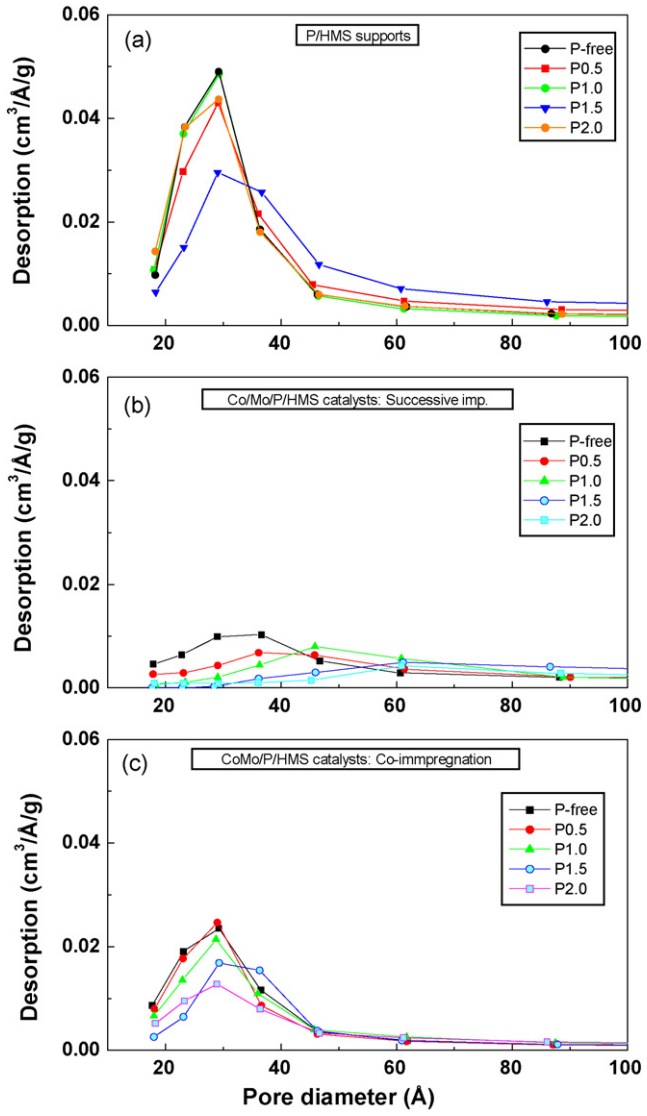

Fig. 2. Pore diameter distribution of supports (a) and calcined catalysts prepared by successive impregnation (b) and co-impregnation (c).

NH_3 profiles of the synthesized materials with varying amounts of phosphate are displayed in Fig. 3. In order to obtain the acid distribution, the experimental TPD curves were fitted by Gaussian distribution analysis (not shown here), in which three peaks were used to represent the weak ($T < 550$ K), medium (550 K $< T <$ 750 K) and strong ($T > 750$ K) acidities, respectively [40]. The presence of phosphate phase on the surface of HMS material led to formation of weak acid sites which amount increased raising P-content in the support. The P(0.5)/HMS material clearly shows two peaks in the low temperature region ($T < 550$ K) which could be related to different nature of the acid sites rather than to changes in textural parameter since BET area remains essentially unchanged along the phosphate range explored. For all P-containing HMS supports, the medium acidity apparently decreased with respect to P-free HMS material. With exception of the P(1.5)/HMS substrate, the other P-containing materials show lower amount of strong acid sites than P-free HMS. The P(1.5)/HMS support shows larger

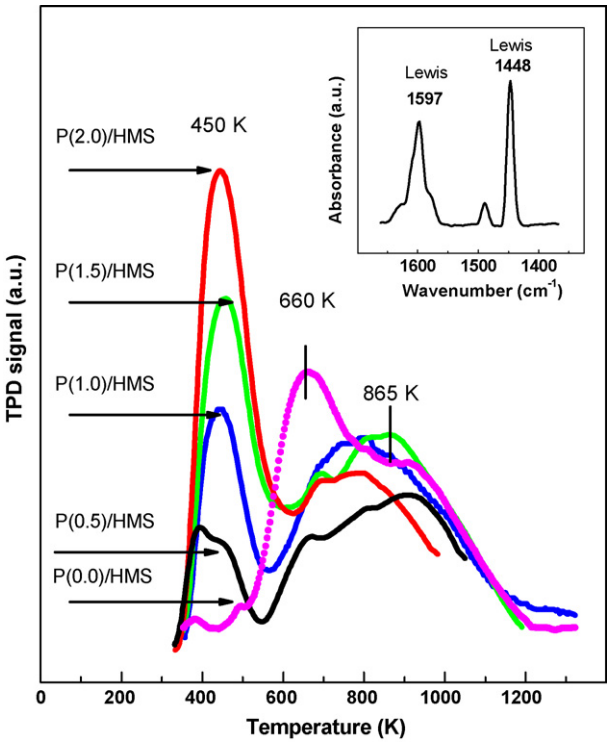

Fig. 3. NH_3-TPD profiles of pure supports. The inlet show the FTIR spectrum of adsorbed pyridine on sulphided CoMo/P(1.5)/HMS catalyst.

amount of strong acid sites than P(2.0)/HMS material although the latter contains larger amount of weak acid sites.

The acid properties of the freshly sulphided catalysts were examined by FTIR of chemisorbed pyridine. As an example, the IR spectrum of the CoMo/P(1.5)/HMS catalyst is presented in inlet of Fig. 3. All catalysts showed two strong bands at ca. 1448 and 1597 cm^{-1} arising from pyridine coordinatively bonded on Lewis acid sites [16,33] and absence of the band at ca. 1550 cm^{-1} ascribed to Brønsted acidity.

3.3. X-ray diffraction (XRD)

The XRD revealed that the incorporation of phosphate on the HMS substrate does not change its structure (XRD patterns not shown here). This is not the case when alumina instead HMS is employed as carrier of the active phases because phosphate reacts to a large extent on the surface layers of the alumina substrate and forms a well dispersed $AlPO_4$ compound [18,33,34]. The reasons for this lies in the fact that the siliceous HMS substrate is much less reactive than alumina and hence phosphate remains deposited as a separate phase on the HMS substrate. Fig. 4 shows the diffractions patterns of the selected oxide Co/Mo and CoMo catalysts. All samples showed the characteristic diffraction peaks associated with the HMS wormhole structure, indicating that the HMS structure does not suffer major changes after deposition of Co and Mo. The XRD patterns of all catalysts display two low intensity peaks at the background of the silica at 26.5° and 23° 2θ. These peaks are assigned to β-$CoMoO_4$ crystallites (JCPDS card 21-868). In addition, the presence of a minor proportion of MoO_3

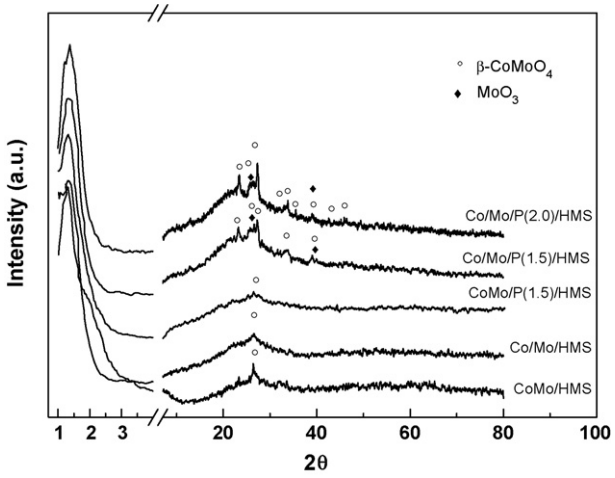

Fig. 4. XRD diffraction profiles of calcined catalysts.

crystallites cannot be precluded. It can also be noted that reflection lines of β-$CoMoO_4$ (and MoO_3) phase are more intense in the sequentially impregnated catalysts on the substrates containing high P-loadings. This finding point out to the presence of larger crystallites of β-$CoMoO_4$ (and MoO_3) phase, which is consistent with the lower BET area of these samples (cf. Fig. 1). For all catalysts, the $Co_3(PO_4)_2$ phase, if exists, appeared to be (X-ray) amorphous.

3.4. UV–vis diffuse reflectance spectra (DRS)

The coordination environment of Co^{2+} and Mo^{6+} ions in the oxide catalysts was studied by UV–vis diffuse reflectance spectroscopy. UV–vis DR spectra of the catalysts prepared by sequential and co-impregnation are compared in Fig. 5. Irrespectively of the impregnation methodology employed, all oxide catalysts displayed similar spectra. The strong band at about 300 nm observed in all spectra can be assigned to charge transfer transition from the oxygen ligands to Mo^{6+} ions in octahedral coordination [41,42]. The visible part of the spectra contains a shoulder at about 400 nm, which is assigned to Co^{2+} in an octahedral coordination [43]. Additionally, a broad band in the region 450–650 nm is observed. Using Gaussian distribution analysis (not shown here), three absorption bands at 446, 489 and 653 nm ascribed to tetrahedral cobalt (II) ions are observed [44–47]. It is suggested that tetrahedral Co^{2+} ions belong to the Co_2SiO_4 phase which is formed at temperatures above 623 K. As stated above, XRD revealed that the β-$CoMoO_4$ phase prevails in the P-containing samples. A similar conclusion can be also derived from DR spectra. Irrespective of the method of catalyst preparation, the intensity of the band at 400 nm is much intense than that 450–650 nm. Because the d–d transition in octahedral coordination is less probable than that in tetrahedral coordination, the difference in the intensity of the bands is possible when the concentration of the octahedral species is much higher than that of the eventually formed tetrahedral species of Co^{2+}.

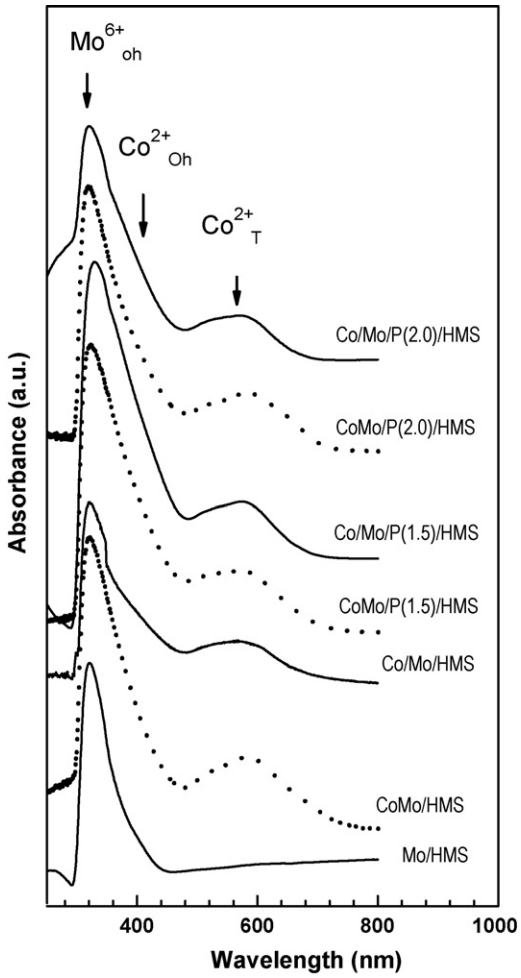

Fig. 5. UV–vis DR spectra of calcined catalysts prepared by sequential impregnation (solid line) and co-impregnation (dotted line). As reference, the DR spectrum of the Mo/HMS catalyst is included. The spectrum of each support was subtracted from the spectrum of the corresponding catalyst.

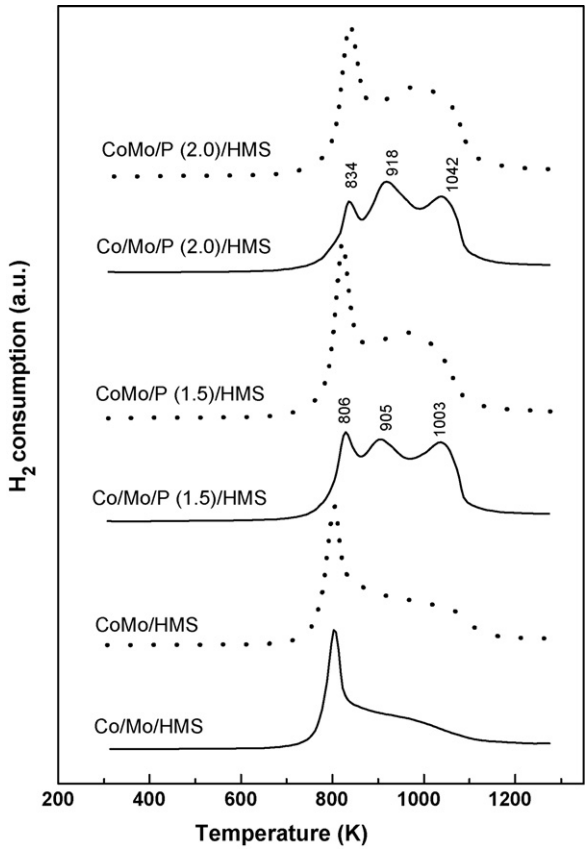

Fig. 6. TPR profiles for oxide catalysts prepared by sequential impregnation (solid line) and co-impregnation (dotted line).

3.5. Temperature-programmed reduction (TPR)

Some clues on the effect of phosphate and preparation method on the catalyst structure can be derived from the reduction profiles of cobalt and molybdenum species. TPR profiles of the P-free and P-containing catalysts prepared by sequential and co-impregnation are presented in Fig. 6. The TPR profiles of high P-content CoMo catalysts prepared by co-impregnation were very different from that of catalysts prepared by sequential impregnation. There is a strong influence of P-loading on the reduction profiles of catalysts prepared by sequential impregnation. All the catalysts show a narrow peak centred at ca. 903 K with a large shoulder extending in the temperature range 839–1113 K. The former peak is indicative of the formation of only one type of species on the catalyst surface. Since this peak is similar to the one reported for $CoMoO_4$ [48,49], it could be inferred that the $CoMoO_4$ phase is formed on all the samples and therefore a strong Co–Mo interaction is expected to be developed in a common crystalline structure. The large hydrogen consumption observed in the temperature range 839–1113 K probably contain peaks belonging to the two-step reduction of MoO_3 ($MoO_3 \rightarrow MoO_2 \rightarrow Mo^0$), which are located at higher temperatures than those of Co species. In agreement with XRD profiles, the amount of reducible Mo oxide species without interaction with the support and/or with cobalt oxide gradually increase upon increasing P_2O_5 loading from 1.5 to 2.0 wt.%. Thus, the reduction profiles of Co/Mo/P(1.5)/HMS and Co/Mo/P(2.0)/HMS catalysts show H_2-consumption peaks at 834, 918 and 1042 K. The P-free catalyst (Co/Mo/HMS) prepared by sequential impregnation shows the lowest reduction temperature among the catalysts studied. For this catalyst, the shift of peak temperature might indicate the high dispersion of cobalt oxide species. Contrary to the catalysts prepared by sequential impregnation, the high P-content catalysts prepared by co-impregnation did not show individual peaks in high temperature region. The narrow peak at 829 K as well as large hydrogen consumption between 873 and 1073 K is due to $CoMoO_4$ species and two steps reduction of Mo^{6+} oxide species interacting strongly with the support, respectively.

Finally, one may note that for all catalysts the molybdenum oxide was so finally dispersed on the supports that a strong metal–support interaction increased the reduction temperature to a broad zone starting from ca. 800 K. In comparison with P-free catalysts, the TPR profile of the P-containing catalysts showed more intense reduction peak in this high temperature region indicating that phosphate increases the total reducibility

of catalysts being this effect more marked in case of catalysts prepared by co-impregnation.

3.6. High-resolution electron microscopy (HRTEM)

The slabs dimension and staking of MoS_2 phase for sulphide CoMo/P(1.5)/HMS and Co/Mo/P(1.5)/HMS catalysts was studied by high resolution electron microscopy. The TEM images of these two representative samples are shown in Fig. 7(a and b), respectively. For both catalysts, typical MoS_2 slabs randomly distributed on the support can be identified from their typical fringes. The distance between two slabs ca. 0.6 nm was in accordance with that expected for crystalline MoS_2. The TEM images of catalyst prepared by co-impregnation (Fig. 7(a)) indicate smaller MoS_2 crystallites (ca. 2.8 nm versus 5.7 nm) and larger stacking (2–7 versus 2–4) than in its homologous prepared by sequential impregnation (Fig. 7(b)). Thus, it can be concluded that the main effect of sequential impregnation is formation of a larger planar MoS_2 slabs which results in a lower dispersion of MoS_2 phase, in good agreement with XPS analyses (see below).

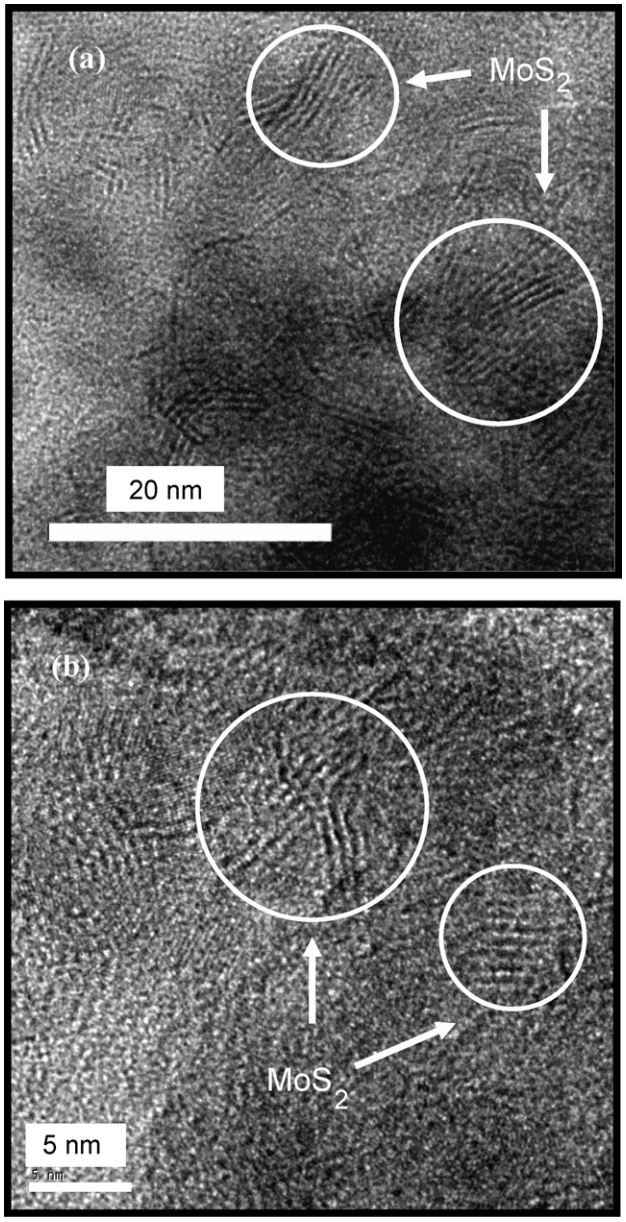

Fig. 7. HRTEM images of fresh sulphided CoMo/P(1.5)/HMS (a) and Co/Mo/P(1.5)/HMS (b) catalysts.

3.7. FTIR of adsorbed NO

The FTIR spectra of the fresh sulphided CoMo/P(1.5)/HMS and Co/Mo/P(1.5)/HMS catalysts are displayed in Fig. 8. As expected from our previous works [50,51], two mayor bands around of 1870 and 1800 cm^{-1} are observed together with a very broad one located at lower frequency region. For the catalyst prepared by co-impregnation, the decomposition of the IR spectra into Gaussian peaks shows the presence of bands around 1877, 1856, 1801, 1787, 1672 and 1618 cm^{-1} whereas for the catalyst prepared by successive impregnation the position of the bands were: 1872, 1852, 1795, 1773, 1680 and 1622 cm^{-1}. The assignments of this bands has been made considering that the spectra of NO chemisorbed on sulphided Co/Al_2O_3 sample shows the bands at 1857 and 1792 cm^{-1} (the symmetric and anti-symmetric stretching vibration modes, respectively, of a dinitrosyl adsorbed on sulphide Co^{2+} sites).

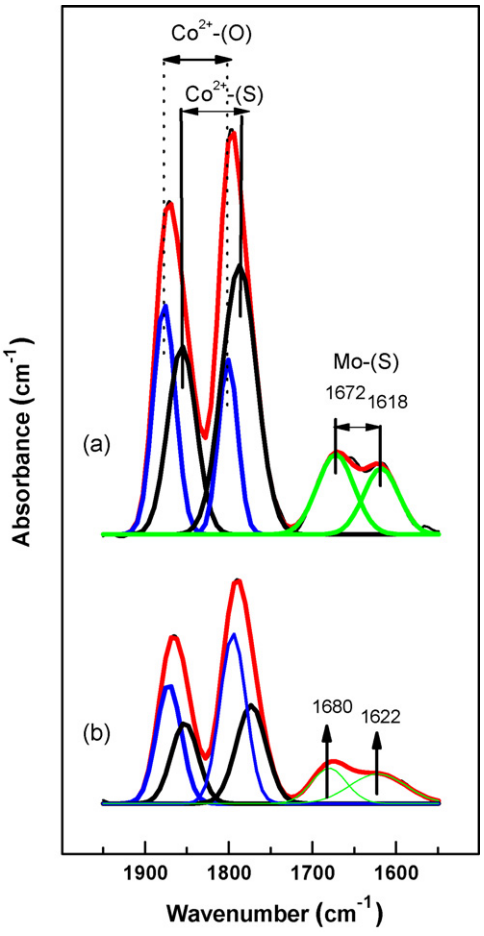

Fig. 8. FTIR spectra of adsorbed NO on sulphided (673 K) samples: CoMo/P(1.5)/HMS (a) and Co/Mo/P(1.5)/HMS (b) catalysts.

Similarly, sulphide Mo/Al_2O_3 catalyst shows the doublet bands around 1740 and 1652 cm^{-1} (the symmetric and anti-symmetric stretching vibrations of NO, respectively, adsorbed on sulphide Mo^{4+} sites) [51]. On this basis, the doublet bands around 1672 and 1618 cm^{-1} was assigned to dinitrosyl species adsorbed on sulphide Mo^{4+} sites, with two different Mo-S environments. Moreover, the low intensity of the former band confirms the location of Co species on the molybdenum sulphide since the presence of non-sulphided Mo species was excluded by XPS measurements discussed below.

For both catalysts, the presence of the absorption bands around 1877 and 1801 cm^{-1} can be due very likely to adsorption on non-sulphided Co^{2+} sites, i.e., Co_2SiO_4 and/or β-$CoMoO_4$, whereas the doublet around 1856 and 1787 cm^{-1} arise from dinitrosyls adsorbed on Co^{2+}-S species. Thus, irrespective of the method of catalyst preparation, these spectra confirm the presence of both sulphide and non-sulphide Co^{2+} species in both samples together with a small contribution of MoS_2 species.

When comparing these spectra of catalyst prepared by co-impregnation with that of sulphide $CoMo/Al_2O_3$ catalyst [51] and the successive-impregnated one, it is clear that the bands of NO adsorbed on MoS_2 sites in the co-impregnated sample is shifted toward lower wavenumber region (from 1680 to 1672 cm^{-1}). However, in good agreement with XPS data discussed below, this shift is so small that one may suppose the formation of a "CoMoS" mixed phase. Additionally, one may to note that for both catalysts the intensities ratio of the bands at around 1680 and 1780 cm^{-1} was similar (0.32 versus 0.28). This may indicate the similar amount of coordinatively unsaturated sites (CUS) formed on MoS_2 phase of both samples.

3.8. Surface analysis of sulphide catalysts

The effect of P incorporation on HMS structure and the impregnation methodology of CoMo on the chemical state of the elements and their relative proportions at the surface of sulphided catalyst were studied by XPS technique. The BE values of the Mo $3d_{5/2}$, Co 2p, P 2p and S 2p core levels are summarized in Table 1. As example, the Mo 3d and Co 2p core-level spectra of sulphided CoMo/P(1.5)/HMS and Co/Mo/P(1.5)/HMS catalysts are shown in Fig. 9(a and b), respectively.

Table 1
Binding energies (eV) of the fresh sulphided (673 K) CoMo catalysts

Catalyst	Mo $3d_{5/2}$	Co $2p_{3/2}$		Si 2p	P 2p	S 2p
		CoS_2	Co^{2+}-O			
Co/Mo/HMS[a]	228.7	778.2 (30)	780.9 (70)	103.0	134.0	162.1
CoMo/HMS[b]	228.6	778.2 (45)	780.8 (55)	103.1	134.1	162.1
Co/Mo/P(1.5)/HMS[a]	228.7	778.2 (34)	780.8 (66)	103.2	134.0	162.2
CoMo/P(1.5)/HMS[b]	228.8	778.3 (54)	780.9 (46)	103.0	134.1	162.1
Co/Mo/P(2.0)/HMS[a]	228.7	778.3 (42)	780.8 (58)	103.2	134.1	162.1
CoMo/P(2.0)/HMS[b]	228.8	778.3 (45)	781.0 (55)	103.2	134.0	162.2

[a] Prepared by sequential impregnation.
[b] Prepared by co-impregnation.

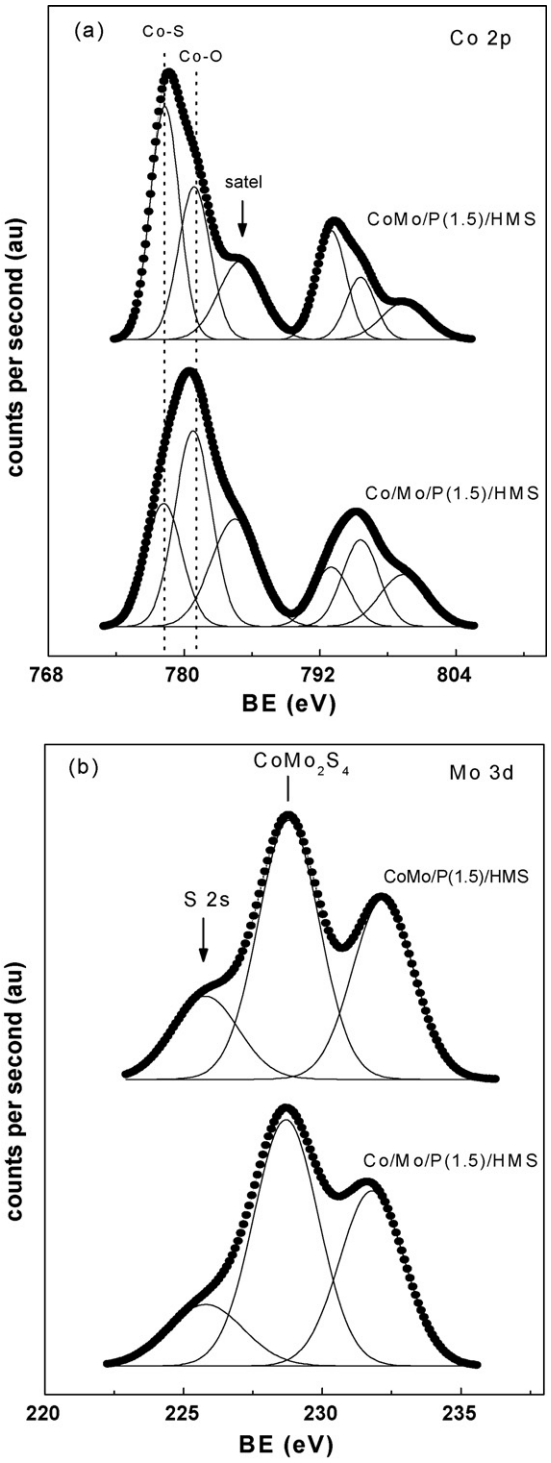

Fig. 9. Co 2p (a) and Mo 3d (b) core-level spectra of the fresh sulphided CoMo/P(1.5)/HMS and Co/Mo/P(1.5)/HMS catalysts.

After sulphidation at 673 K, all sulphided CoMo catalysts showed the S 2p peak with binding energy at 161.2 ± 0.1 eV, which is characteristic of S^{2-} ions. Additionally, the P 2p peak at 134.0 eV is indicative of phosphate species [31]. For all catalysts, the Mo $3d_{5/2}$ core level spectra showed BE values at 228.7–228.8 eV, which is close to that of $CoMo_2S_4$ species (228.7 eV) [52]. No other peaks placed at higher binding

Table 2
Surface atomic ratios of the fresh sulphided (673 K) catalysts[a]

Catalyst	Mo/Si atomic	Co/Si atomic	Co/Si atomic (CoS_2)	Co/Mo atomic	P/Si atomic	S/(Mo + Co) atomic
Co/Mo/HMS[b]	0.013 (0.072)	0.007 (0.035)	0.0022	0.57	0.0	1.26
CoMo/HMS[c]	0.017 (0.072)	0.011 (0.035)	0.0050	0.66	0.0	1.39
Co/Mo/P(1.5)/HMS[b]	0.018 (0.073)	0.011 (0.036)	0.0037	0.61	0.023	1.54
CoMo/P(1.5)/HMS[c]	0.020 (0.073)	0.013 (0.036)	0.0071	0.66	0.031	1.77
Co/Mo/P(2.0)/HMS[b]	0.015 (0.074)	0.009 (0.036)	0.0037	0.58	0.034	1.62
CoMo/P(2.0)/HMS[c]	0.017 (0.074)	0.011 (0.036)	0.0048	0.62	0.037	1.67

[a] Theoretical bulk atomic ratio, as calculated from nominal metal contents, are given in parenthesis.
[b] Prepared by sequential impregnation.
[c] Prepared by co-impregnation.

energies belonging to oxy-sulphide species, i.e., $MoO_2S_2^{2-}$, or unreduced Mo^{6+} ions were found. On the contrary, the Co 2p core-level spectra of sulphided catalysts display two contributions: a minor one at 778.2–778.3 eV indicative of CoS_2 species [52], and another at 780.8–781.0 eV indicative of Co^{2+} ions in the Co_2SiO_4 phase. In good agreement with XRD data of the calcined CoMo catalysts, the latter peak confirmed that during calcination, a fraction of Co is lost at the HMS interface by forming Co_2SiO_4 phase by solid state reaction.

In addition, the calculation of the difference between the Co $2p_{3/2}$ binding energy and the Mo 3d binding energy was performed [53]. For all catalysts this difference was 549.5–549.6 eV, which is relatively far from the value of 550.0 eV reported in literature for catalysts possessing the cobalt atoms located in a decoration position of MoS_2 phase [53]. Moreover, the BE of Co $2p_{3/2}$ core level was found to be much lower than those expected for Co located in the catalytically active "CoMoS" phase [54,55].

Table 2 compiles the Mo/Si, Co/Si, Co/Mo and P/Si surface atomic ratios of fresh sulphided catalysts. Irrespectively of the P-content, the co-impregnated samples display not only a slightly higher sulphidation degree of Co species but also somewhat better surface exposure of Co and Mo phases than their sequentially impregnated counterparts. In addition, the CoMo/P(1.5)/HMS sample showed a little better surface exposure of Mo and Co species than the other catalysts studied. Considering the S/(Mo + Co) atomic ratio, which is a measure of the extent of sulphidation of CoMo phases (Table 2), the following trend can be established: CoMo/P(1.5)/HMS > CoMo/P(2.0)/HMS > Co/Mo/P(2.0)/HMS > Co/Mo/P(1.5)/HMS ≫ CoMo/HMS > Co/Mo/HMS. Thus, irrespectively of the catalyst preparation method employed, the presence of P_2O_5 species on the support surface has positive effect on the sulphidation degree of Mo and Co species being this effect larger for the catalysts prepared by co-impregnation.

3.9. Catalytic properties

The catalysts were tested in the HDS reaction of DBT in a batch reactor under hydrogen pressure of 3.8 MPa at 623 K. The commercial $CoMo/Al_2O_3$ catalyst was used as reference. DBT conversion and selectivity of catalysts as a function of P_2O_5 loading are presented in Fig. 10(a and b), respectively. Whichever the methodology employed in catalyst preparation, both P-free samples showed very close activity at reaction time of 5 h (see Fig. 10(a)). On the contrary to P-free samples, the presence of phosphate on the HMS substrate determines different catalytic behaviours depending on the way by which

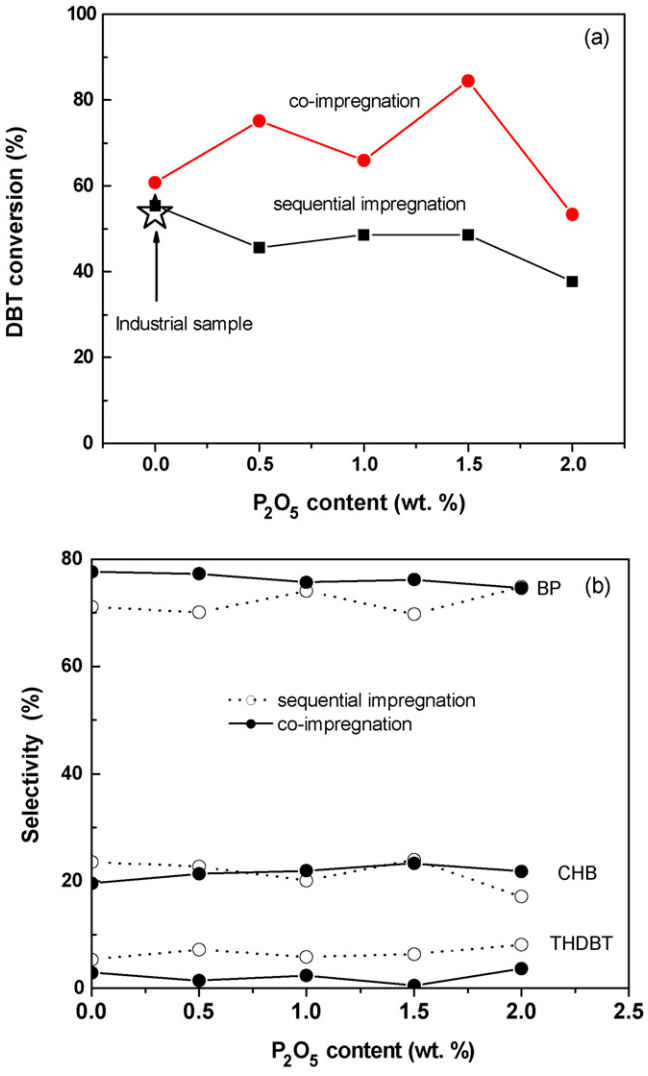

Fig. 10. Total DBT conversion (a) and product distribution (b) at reaction time of 5 h in the HDS of DBT over CoMo/P/HMS catalysts as a function of P_2O_5 content. The DBT conversion data of an industrial sample is included.

Table 3
Comparison of the selectivities during HDS of DBT over Co/Mo/HMS and CoMo/P(1.5)/HMS catalysts with those of commercial $CoMo/Al_2O_3$

Catalyst	(%)				DBT conversion (%)/(reaction time (h))
	DBT	THDBT	BP	CHB	
Co/Mo/HMS[a]	46.2	3.1	38.3	12.4	53.8 (5.0)
CoMo/P(1.5)/HMS[b]	46.5	2.0	40.4	11.1	53.5 (2.5)
$CoMo/Al_2O_3$	46.4	3.4	35.0	15.2	53.6 (5.0)

[a] Prepared by sequential impregnation.
[b] Prepared by co-impregnation.

CoMo phases were incorporated being the catalysts prepared by co-impregnation clearly more active than those prepared by sequential impregnation. However, for catalysts prepared by co-impregnation an increase in activity was observed for the P_2O_5 content up to 1.5 wt.% and then the decrease in activity occurs. Similarly, the limited increase in DBT HDS activity was reported by Kwak et al. [16] for the P-modified CoMo/γ-alumina catalysts, but the limit of P_2O_5 for γ-alumina was much lower than in case of the siliceous HMS material (0.5 P_2O_5 wt.% versus 1.5 P_2O_5 wt.%).

For all catalysts, the reaction products identified by GC were biphenyl (BP), cyclohexylbenzene (CHB) and tetrahydrodibenzothiophene (THDBT) (Fig. 10(b)). Hydrocracking products, such as benzene and cyclohexane, were not detected. The time course of product distribution (did not shown here) demonstrated that CHB increased with reaction time. Such increase might indicate that CHB is produced mainly from THDBT. In Table 3 are compared the selectivities of the Co/Mo/HMS and CoMo/P(1.5)/HMS catalysts with those of a commercial $CoMo/Al_2O_3$ sample obtained at the same DBT conversion (ca. 54%). Both home-made catalysts and commercial one presented the same selectivity. Thus, product distribution did not depend on the sequence of metal incorporation and presence of phosphate. Scheme 1 shows the DBT HDS reaction pathways derived from product distribution. HDS reaction of DBT proceeds through two different pathways, a hydrogenation (HYD) route and a direct desulphurization route (DDS). For all catalysts, including the commercial one, BP was the main product (DDS route) and significant amounts of CHB (HYD route) were also formed.

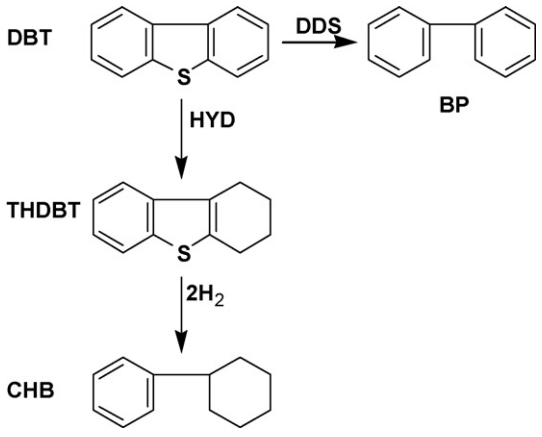

Scheme 1. Simplified dibenzothiophene HDS reaction scheme.

Though CHB is mainly produced from the transformation of THDBT, selectivity did not depend on the P_2O_5 content.

As all activity batch reactions were extended for 5 h, it is not possible to get reliable information on catalyst deactivation. Our unpublished TGA results on coke formation on the CoMo/P/HMS catalysts used in reaction of HDS of 4,6DMDBT indicate that the deactivation of those systems is a complex process [56]. Thus, contrary to the Al_2O_3-supported catalysts [57–59], incorporation of phosphate into HMA material leads to coke formation being the P-free sample the one which showed about two times less coke formation than the other P-containing ones. Since the amount of coke formed did not follow the trend of P_2O_5 content in the catalysts, this indicates that coke formation on those systems is a complex process. A more detailed study on the catalyst deactivation is in progress [56].

4. Discussion

In this study the morphology and activity of the CoMo/P(*x*)/HMS catalysts depend on the presence of phosphate species on the surface of HMS carrier as well as on the catalyst preparation method employed. The better catalytic behaviour of CoMo/P(*x*)/HMS catalysts prepared by co-impregnation with respect to Co/Mo/P(*x*)/HMS counterparts prepared by successive impregnation seems to be linked with the morphology of the Co/Mo phases formed after calcination/sulphidation. This connection can be understood by considering that the active phases formed after sulphidation at 673 K have their origin in the oxide precursors. Thus, the surface properties of P(*x*)/HMS substrates and the corresponding CoMo-loaded oxide catalyst precursors are discussed in a first instance.

With respect to phosphate incorporation, the TPD-NH_3 measurements confirmed that phosphate induced changes in the acid sites distribution of P(*x*)/HMS supports. After calcination at 813 K, the P(*x*)/HMS substrates showed a lower quantity of medium and strong strength acid sites and a larger quantity of weak acid sites than the P-free HMS sample (Fig. 3). Thus, in line with previous work [60], the distribution of surface OH groups in supports is largely modified in the presence of P_2O_5 phase on the support surface. Since the surface OH groups are particularly important for the distribution of Mo species and the type of Mo species formed, it has been proposed that a large amount of P_2O_5 phase (above 1.5 wt.%) on the catalyst surface influenced negatively on the Mo distribution because most of the –OH groups can be removed upon interaction with phosphate groups. In other words, the presence of phosphate

alters the isoelectric point of the HMS surface (pH ca. 3). As in the sequential impregnation of P(*x*)/HMS supports were firstly impregnated with molybdate solutions, a phosphomolybdate such as $P_2Mo_5O_{26}^{6-}$ might be formed. During adsorption on the HMS surface these complexes decompose because of the preferential adsorption of the molybdate ions on basic sites and of the phosphate ions adsorption on more acidic sites [61]. After calcination in air at 773 K, Mo-O-Mo species, and even MoO_3 crystallites, are formed on the support surface. Then impregnation of Mo/HMS catalysts with cobalt salt solution results in the formation of Co-species in the close vicinity of Mo-species.

On the other hand, a simple electrostatic model may account for the formation of β-$CoMoO_4$ phase in the co-impregnated samples. During impregnation of P-modified HMS substrates with the molybdate solution it is likely that the surface of plain P/HMS support becomes positively charged (presence of P-OH groups). In parallel, the following ionic equilibrium occurs in the molybdate solution:

$$Mo_7O_{24}^{7-} + 4H_2O \leftrightarrow 7MoO_4^{2-} + 8H^+$$

This means that the adsorption of polymolybdate ($Mo_7O_{24}^{7-}$) ions should be favoured by low pH. In such case, the polymolybdate ions adsorbed through electrostatic forces with OH groups of the support surface may then facilitate the adsorption of positively charged Co^{2+} ions on its neighbourhood. Such a topology would be particularly suited to formation of a β-$CoMoO_4$ phase upon calcination, as confirmed by XRD and TPR measurements. In favour of this interpretation is the formation of a very low quantity of β-$CoMoO_4$ phase in the phosphorous-free sample prepared by co-impregnation.

The UV–vis DR spectra of all calcined Co/Mo/P(*x*)/HMS samples revealed that Co^{2+} ions are mainly octahedrally coordinated by oxide ions. This result is consistent with the observation by XRD of β-$CoMoO_4$ phase whose proportion was found to increase upon raising the phosphate content on the HMS substrate. A similar effect has previously been reported for alumina-supported catalysts [62]. Upon sulphidation at 673 K, both Co sulphide and $CoMo_2S_4$ phases are developed and their surface exposure depends on the phosphate loading. The lower exposure of sulphide Mo and Co species found in the P-free sample suggests that agglomeration of Co sulphide and $CoMo_2S_4$ phases takes place along sulphidation. The combined XPS and activity measurements indicate that DBT conversion increases almost linearly with an increase of the surface exposure of CoS_2 species (Fig. 11), with the only exception of the P-free Co/Mo/HMS sample. Indeed, the sequentially impregnated catalysts displaying a lower Co/Si ratio are less active than the corresponding co-impregnated counterparts. The comparison of bulk and surface exposure of Co/Mo species in the catalysts (Table 2) indicates that, irrespectively of the method of catalyst preparation employed, all catalysts possess active phases located mainly within the inner pore structure. This agrees with the N_2 adsorption–desorption data which show a large decrease of BET surface area after Co and Mo incorporation (Fig. 1). Such decrease is larger in the catalysts prepared by sequential impregnation than on their counterparts

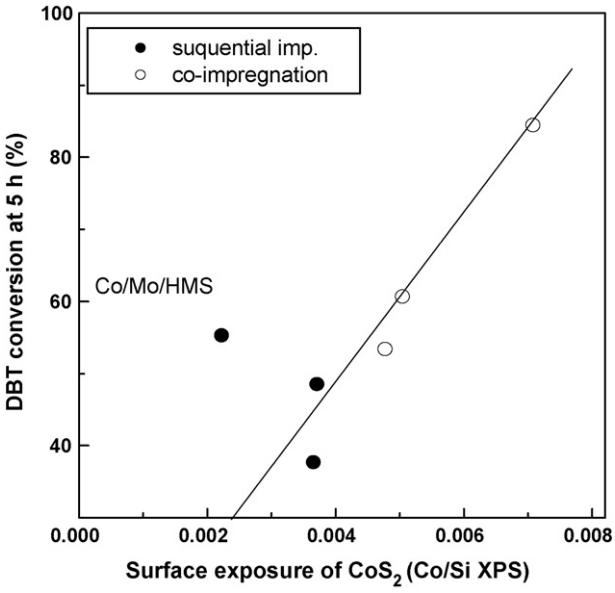

Fig. 11. DBT conversion vs. surface exposure of CoS_2 species as determined from XPS of sulphided CoMo catalysts.

prepared by co-impregnation. This might indicate that the correlation observed between surface exposure of cobalt sulphide and catalyst activity is due to a preferential location of the active components on the outer surface. For all sulphided catalysts, the FTIR spectra of adsorbed pyridine confirmed the presence of only Lewis acidity and this increases with an increase in P_2O_5 content. This contrasts with the increase of Brønsted acidity reported previously for sulphided CoMo/Al_2O_3 catalysts with a large P-content (the single $P(OH)_2$-O-Al occurs at high P concentration on alumina, and hence the Brønsted acidity of the catalyst increases) [16]. Since this is not case of our siliceous HMS material modified by P, it can be concluded that the dispersion of active phase achieved in our P-containing HMS systems is much better than that reported for alumina-supported catalysts [16].

An examination of catalyst structures and performance indicate that several factors have to be considered to explain the enhancement of HDS activity of P-loaded HMS supports to which CoMo phases were incorporated by co-impregnation. These include: (i) the larger BET surface area (Table 1); (ii) the enhancement of reducibility of oxide precursors (TPR data); (iii) improved sulphidation degree of cobalt species (see percentage of CoS_2 given Table 1); (iv) improved surface exposure of the active phases, as it was already observed for P-modified CoMoS/Al_2O_3 [16] (Table 2); (v) formation of stacked molybdenum layers easier to sulphide (derived from HRTEM); (vi) the formation of a larger amount of the coordinatively unsaturated sites (CUS) in MoS_2 phases. The sulphide co-impregnated CoMo/P(1.5)/HMS sample was found to be the most active among the catalyst studied (Fig. 10(a)). Taking into account the XPS data of freshly sulphided catalysts, this is because the Mo and Co surface exposure was higher for the P(1.5)/HMS support (Table 2). Similar optimum in DBT HDS activity due to optimized dispersion of molybdenum

species was reported for CoMo/P/Al_2O_3 catalysts modified by P [24]. However, the limit of the P_2O_5 content on the alumina was found to be much lower than in case of our HMS catalysts (0.5 wt.% versus 1.5 wt.%). For the larger P_2O_5 content on alumina, the decrease in activity was explained in terms of the formation of relatively stable Co-Mo-P phase [24]. In this study, the comparison of HRTEM micrographs of sulphide co-impregnated CoMo/P(1.5)/HMS sample (Fig. 7(a)) with its sequentially impregnated counterpart (Co/Mo/P(1.5)/HMS) (Fig. 7(b)) revealed the presence of smaller MoS_2 slabs (ca. 2.8 nm versus 5.7 nm) and larger stacking (number of layers 2–7 versus 2–4) on the former. The larger columns of MoS_2 phase, presumably decorated by Co atoms at the edges, are more active than smaller ones, still having bigger basal sections. Thus, it appears that the probability of formation of S-vacancies, which are known to be active in HDS reaction, is favoured on the sulphide co-impregnated CoMo/P(1.5)/HMS sample. This catalyst showed larger activity in the HDS reaction of DBT than the commercial CoMo/Al_2O_3 catalyst (84.5% versus 53.6% conversion), still containing a higher metal-loading.

5. Conclusions

This study revealed that the morphology of the sulphide phases depends on the method of catalyst preparation as well as on the presence of P_2O_5 species on the surface of HMS support being the former factor more important than the latter. For the oxide catalysts, TPR results showed that both phosphate and co-impregnation increases the total reducibility of catalysts. Irrespectively of the sequence of impregnation, all sulphide catalysts showed only Lewis acidy and this increases after phosphate incorporation. The catalysts prepared by sequential impregnation of Co and Mo salts on the P(x)/HMS supports were less active in hydrodesulphurization of dibenzothiophene than catalysts prepared by co-impregnation. Contrary to sequential impregnation, the addition of phosphate to HMS support up to 1.5 wt.% of P_2O_5 is positive when catalysts were prepared by co-impregnation. Incorporation of Co and Mo salts by co-impregnation on the P(1.5)/HMS substrate led to a much more active catalyst (84.5% conversion) in the HDS reaction of DBT than the commercial CoMo/Al_2O_3 catalyst (53.6%), still containing a higher metal-loading. As revealed by photoelectron spectroscopy, this difference in catalytic performance is linked with the larger surface exposure of both Co and Mo sulphide phases in co-impregnated catalysts. In addition, comparison of HRTEM micrographs for the most active CoMo/P(1.5)/HMS catalyst and its sequentially impregnated Co/Mo/P(1.5)/HMS counterpart revealed smaller MoS_2 slabs (ca. 2.8 nm versus 5.7 nm) and larger stacking (number of layers 2–7 versus 2–4).

Acknowledgements

The authors would like to express their gratitude to PAPIIT, DGAPA, UNAM, México, Project IN118002, Conacyt project 40118-Y, for financial support. The authors are grateful to Ing. M. Hernández, Dr. J. Arenas and Dr. Lardizabal for technical assistance.

References

[1] EP directive 2003/17/EC, Off. J. Eur. Union L 76, 46 (2003) 10.
[2] J.J.L. Heinerman, A.J. van Hengstum, M. de Mind, US Patent 5246569, to Akzo N.V. (1993).
[3] W.S. Millman, US Patent 4392985, to Union Oil Co. of California (1983).
[4] H.D. Simpson, R.L. Richardson, K. Baron, US Patent 4500424, to Union Oil Co. of California (1985).
[5] D. Chadwick, D.W. Aitchinson, R. Badilla-Ohlbaum, L. Joseffson, Stud. Surf. Sci. Catal. 16 (1983) 323.
[6] G. Muralidhar, F.E. Massoth, J. Shabtai, J. Catal. 85 (1984) 44.
[7] J.M. Lewis, R.A. Kydd, J. Catal. 136 (1992) 478.
[8] P. Atanasova, T. Halachev, J. Uchytil, M. Kraus, Appl. Catal. A: Gen. 38 (1988) 235.
[9] J.L.G. Fierro, A. López Agudo, N. Esquivel, R. López Cordero, Appl. Catal. 48 (1989) 353.
[10] R. López Cordero, N. Esquivel, J. Lazaro, J.L.G. Fierro, A. López Agudo, Appl. Catal. A: Gen. 48 (1989) 341.
[11] S.M.A.M. Bouwens, J.P.R. Vissers, V.H.J. De Beer, R. Prins, J. Catal. 112 (1988) 401.
[12] S. Eijsbouts, L. Van Gruijthuijsen, J. Volmer, V.H.J. De Beer, R. Prins, Stud. Surf. Sci. Catal. 50 (1989) 79.
[13] S. Eijsbouts, J.N.M. Van Gestel, J.A.R. Van Veen, V.H.J. De Beer, R. Prins, J. Catal. 131 (1991) 412.
[14] R. Iwamoto, J. Grimblot, Stud. Surf. Sci. Catal. 106 (1997) 195.
[15] J.A.R. Van Veen, H.A. Colijn, P.A.J.M. Hendriks, A.J. Van Welsenes, Fuel Proc. Tech. 35 (1993) 137.
[16] C. Kwak, Mi. Young Kim, K. Choi, S. Heup Moon, Appl. Catal. A: Gen. 185 (1) (1999) 19.
[17] P. Marchaud, J.L. Lemberton, G. Pérot, Appl. Catal. A: Gen. 169 (1998) 343.
[18] W.R.A.M. Robinson, J.N.M. van Gestel, T.I. Koranyi, S. Eijsbouts, A.M. van der Kraan, J.A.R. van Veen, V.H.J. de Beer, J. Catal. 161 (1996) 539.
[19] C.V. Caceres, J.L.G. Fierro, M.N. Blanco, H.J. Thomas, Appl. Catal. 10 (1984) 333.
[20] A. Morales, M.M. Ramirez de Agudelo, F. Hernandez, Appl. Catal. 41 (1988) 261.
[21] G.A. Michelson, U.S. Pats., 3,749,663; 3,755,196; 3,755,150; 3,755,148; 3,749,664 (1973).
[22] L. Hilfman, U.S. Pat., 3,617,528 (1971).
[23] T.I. Korányi, Appl. Catal. A: Gen. 239 (2003) 253.
[24] C.W. Fitz, H.F. Rase, Ind. Eng. Chem. Prod. Res. Dev. 22 (1983) 40.
[25] P.J. Mangnus, A.D. van Langeveld, V.H.J. De Beer, J.A. Moulijn, Appl. Catal. 68 (1991) 161.
[26] P.J. Mangnus, J.A.R. Van Veen, S. Eijsbouts, V.H.J. De Beer, J.A. Moulijn, Appl. Catal. 61 (1990) 99.
[27] J.C. Edwards, P.D. Ellis, Langmuir 7 (1991) 2117.
[28] H. Kraus, R. Prins, J. Catal. 170 (1997) 20.
[29] T. Chiranjeevi, P. Kumar, M.S. Rana, G. Murali Dhar, T.S.R. Prasada Rao, J. Mol. Catal. A: Chem. 181 (1–2) (2002) 109.
[30] T. Chiranjeevi, P. Kumar, S.K. Maity, M.S. Rana, G. Murali Dhar, T.S.R. Prasada Rao, Micropor. Mesopor. Mater. 44 (2001) 547.
[31] B. Pawelec, S. Damyanova, R. Mariscal, J.L.G. Fierro, I. Sobrados, J. Sanz, L. Petrov, J. Catal. 223 (2004) 86–97.
[32] T.A. Zepeda, J.L.G. Fierro, B. Pawelec, R. Nava, T. Klimova, G.A. Fuentes, T. Halachev, Chem. Mater. 17 (2005) 4062.
[33] T.A. Zepeda, T. Halachev, B. Pawelec, R. Nava, T. Klimova, G.A. Fuentes, J.L.G. Fierro, Catal. Comm. 7 (2006) 33.
[34] T.A. Zepeda, B. Pawelec, J.L.G. Fierro, T. Halachev, J. Catal. 242 (2) (2006) 254.
[35] S. Rojagopal, H.J. Marini, J.A. Marzari, R. Miranda, J. Catal. 147 (1994) 417.
[36] V. Zuzaniuk, R. Prins, J. Catal. 219 (2003) 85.
[37] W. Zhang, M. Froba, J. Wang, P.T. Tanev, T.J. Pinnavaia, J. Am. Chem. Soc. 118 (1996) 9164.

[38] C.D. Wagner, W.M. Riggs, L.E. Davis, J.F. Moulder, G.E. Muilenberg, Handbook of X-ray Photoelectron Spectroscopy, Perkin Elmer Corp., 1979.
[39] S. Brunauer, P.H. Emmett, E. Teller, J. Am. Chem. Soc. 60 (1938) 309.
[40] V.L. Barrio, P.L. Arias, J.F. Cambra, B. Güemez, J.M. Campos-Martin, B. Pawelec, J.L.G. Fierro, Appl. Catal. A: Gen. 248 (2003) 211.
[41] R.A. Schoonheydt, in: F. Delannay (Ed.), Characterization of Heterogeneous Catalysts, Marcel Dekker, New York, 1984, pp. 125–160.
[42] M. Fournier, C. Louis, M. Che, P. Chaquin, D. Masure, J. Catal. 119 (1989) 400.
[43] H. Kasper, Monatsh. Chem. 98 (1967) 2104.
[44] P. Gajardo, P. Grange, B. Delmon, J. Phys. Chem. 83 (1979) 1771.
[45] S. Fernandez, J.L. Pizarro, J.L. Lezama, Int. J. Inorg. Mater. 3 (2001) 331.
[46] M. Zayat, D. Levy, Chem. Mater. 12 (2000) 2763.
[47] H.K. Matralis, Ch. Papadopoulou, A. Lycourghiotis, Appl. Catal. A: Gen. 116 (1994) 221.
[48] K. Segawa, K. Takahashi, S. Satoh, Catal. Today 63 (2000) 123.
[49] K.M. Reddy, C. Song, Catal. Today 31 (1) (1996) 137.
[50] B. Pawelec, R. Navarro, J.L.G. Fierro, P.T. Vasudevan, Appl. Catal. A: Gen. 168 (1998) 205.
[51] A. Arteaga, J.L.G. Fierro, F. Delanny, B. Delmon, Appl. Catal. A: Gen. 26 (1986) 227.
[52] D. Briggs, M.P. Seah (Eds.), Practical Surface Analysis. Auger and X-ray Photoelectron Spectroscopy, Wiley/Salle and Sauerländer, New York, 1990, p. 607.
[53] I. Alstrup, I. Chorkendoref, R. Candia, B.S. Clausen, H. Topsoe, J. Catal. 77 (1982) 397.
[54] Y. Okamoto, T. Kubota, Catal. Today 86 (2003) 31.
[55] J.J. Lee, H. Kim, J.H. Koh, S.H. Ara Jo, Moon, Appl. Catal. B: Environ. 58 (2005) 91.
[56] R. Nava, B. Pawelec, J.L.G. Fierro, unpublished results.
[57] S.K. Maity, J. Ancheyta, L. Soberanis, F. Alonso, Appl. Catal. A: Gen. 253 (2003) 125–134.
[58] J.M. Lewis, R.A. Kydd, P.M. Boorman, P.H. van Rhyn, Appl. Catal. 84 (1992) 103.
[59] A. Spojakina, S. Damyanova, L. Petrov, Z. Vit, Appl. Catal. 56 (1989) 163.
[60] C.V. Cáceres, J.lG. Fierro, J. Lázaro, A. López Agudo, J. Soria, J. Catal. 122 (1990) 113.
[61] W.C. Cheng, N.P. Luthra, J. Catal. 109 (1988) 163.
[62] P. Atanasova, T. Halachev, Appl. Catal. A: Gen. 108 (1994) 123.